

# The *c*-axis length and phase transition temperature change in an epitaxial PbTiO<sub>3</sub> thin film grown on a SrTiO<sub>3</sub>(001) substrate by metal–organic chemical vapour deposition

L Shun, Y-F Chen, T Yu, J-X Chen and N-B Ming

National Laboratory of Solid State Microstructures and Centre for Advanced Studies in Science and Technology of Microstructures, Nanjing University, Nanjing 210093, People's Republic of China

Received 24 January 1995, in final form 11 April 1995

**Abstract.** The room-temperature and high-temperature  $\theta$ - $2\theta$  x-ray diffraction patterns of the PbTiO<sub>3</sub> thin films grown on SrTiO<sub>3</sub>(001) substrates by metal–organic chemical vapour deposition under reduced pressure show that the epitaxial PbTiO<sub>3</sub> thin film has a smaller *c*-axis length and a higher phase transition temperature than does the bulk material. The coexistence of *a* and *c* domains has also been found through the changing temperature x-ray diffraction pattern of the as-grown film. Taking the additional strain items into consideration the original Landau–Ginzburg–Devonshire form of the elastic Gibbs free energy of the PbTiO<sub>3</sub> thin film is different from that of the bulk material, upon this, a relationship between the phase transition temperature and *c*-axis strain in the epitaxial film has been proposed. The reason for the *c*-axis length shortening has been discussed.

## 1. Introduction

The applications of ferroelectric materials in non-volatile memories, pyroelectric, piezoelectric and electro-optic devices have stimulated interest in preparing high-quality ferroelectric thin films in recent years [1–3]. PbTiO<sub>3</sub> with a large spontaneous polarization, small dielectric constant, small coercive field, high Curie temperature (490 °C) and perfect chemical stability has been proved to be an appropriate material. Among the various film preparation techniques, metal–organic chemical vapour deposition (MOCVD) has been well developed in preparing device-quality thin films and superlattices of compound semiconductors since 1968 [4], and it has recently been used to prepare oxide ferroelectric thin films including PbTiO<sub>3</sub> and PZT. This technique has overcome some disadvantages of the most widely used sputtering method, namely the low deposition rate, the generation of surface defects and the composition change between the film and the target. Phase-pure perovskite PbTiO<sub>3</sub> films have been obtained on fused quartz [5], silica and Pt-coated alumina [6] substrates, and epitaxial PbTiO<sub>3</sub> films have also been obtained on MgO(001) [7, 8], KTaO<sub>3</sub>(001) [9], LaAlO<sub>3</sub>(001) [10] and SrTiO<sub>3</sub>(001) [11–13] single-crystal substrates. *c*-axis length shortening has been reported in PbTiO<sub>3</sub> thin films on a MgO substrate by Bai *et al* [14], on a SrTiO<sub>3</sub> substrate by de Keijser *et al* [11] and on LaAlO<sub>3</sub> by Chen *et al* [10]. A phase transition temperature upshift has been reported by Iijima *et al* [15] for PbTiO<sub>3</sub> thin films prepared by the RF-magnetron sputtering method on a MgO substrate. In this paper, both these phenomena have been found in epitaxial PbTiO<sub>3</sub> thin films deposited on SrTiO<sub>3</sub> substrate by MOCVD, and a phenomenological theory is proposed to give the relationship between the two parameters.

## 2. Experiment

PbTiO<sub>3</sub> thin films were grown in a horizontal MOCVD apparatus which has been described in detail in our earlier report [16]. Purified titanium isopropoxide (TIP) and tetraethyl lead (TEL) were used as the metal-organic precursors, and N<sub>2</sub> was the carrier gas; the optimum growth conditions are presented in table 1.

Table 1. Typical growth conditions.

Substrate	SrTiO <sub>3</sub> (001)
Substrate temperature (°C)	≈ 650
Reactor pressure (Torr)	12.0
Carrier gas	N <sub>2</sub>
T <sub>TIP</sub> (°C)	65
T <sub>TEL</sub> (°C)	35
TEL carrier flow rate (sccm)	≈ 100
TIP carrier flow rate (sccm)	≈ 50
O <sub>2</sub> flow rate (sccm)	≈ 100

Mirror-smooth pale-yellow PbTiO<sub>3</sub> thin film was obtained on the SrTiO<sub>3</sub>(001) substrate. Using a surface profilometer, the film thickness was measured to be about 2500 Å. Scanning electron microscopy (SEM) showed that the as-grown PbTiO<sub>3</sub> thin film was dense and had no obvious defects. The  $\theta$ -2 $\theta$  x-ray diffraction (XRD) scan pattern of the film is shown in figure 1. Because the *a*-axis length of PbTiO<sub>3</sub> (3.904 Å) is almost the same as the lattice constant of SrTiO<sub>3</sub> (3.905 Å) at room temperature, (100) reflections of PbTiO<sub>3</sub> and SrTiO<sub>3</sub> could not be separated from each other in the normal XRD measurement. The *c*-axis constant of PbTiO<sub>3</sub> determined by these reflections was 4.102 Å, which is much smaller than that for bulk PbTiO<sub>3</sub> (4.150 Å). The epitaxial nature of the film was proved by a  $\phi$  scan XRD pattern [16]. The phase transition process of the PbTiO<sub>3</sub> thin film was also investigated by the XRD technique. The sample is placed in an electric furnace and surrounded by a Pt resistance thread to create a uniform temperature field; a thermocouple was fixed on the back of the sample for temperature measurement. The rates of heating and cooling were kept at 4°C min<sup>-1</sup>. Figure 2 shows the profile near the (002) peak of PbTiO<sub>3</sub>; it was not until 470°C that the (200) peak of PbTiO<sub>3</sub> could be found separating from the (002) peak of the SrTiO<sub>3</sub> substrate. A phase transition from a tetragonal to a cubic structure was observed at about 515°C and the reverse process occurred at 507°C. Meanwhile figure 3 shows the lattice parameter versus temperature plot; the *a*-axis length changed almost the same way in the heating and cooling cycles without the hysteresis that could be found in the *c*-axis lattice constant.

## 3. Calculation and discussion

To establish a mathematical relationship between the *c*-axis length and the phase transition temperature, a phenomenological theory was proposed according to the Landau-Ginzburg-Devonshire formula; the elastic Gibbs free energy of PbTiO<sub>3</sub> can be written in the following form [17-20] when the non-zero coefficients of the energy function are limited due to the symmetry of the paraelectric phase (*m3m*):

$$\Delta G = \alpha_1(P_1^2 + P_2^2 + P_3^2) + \alpha_{11}(P_1^4 + P_2^4 + P_3^4) + \alpha_{12}(P_1^2 P_2^2 + P_2^2 P_3^2 + P_3^2 P_1^2) + \alpha_{111}(P_1^6 + P_2^6 + P_3^6)$$

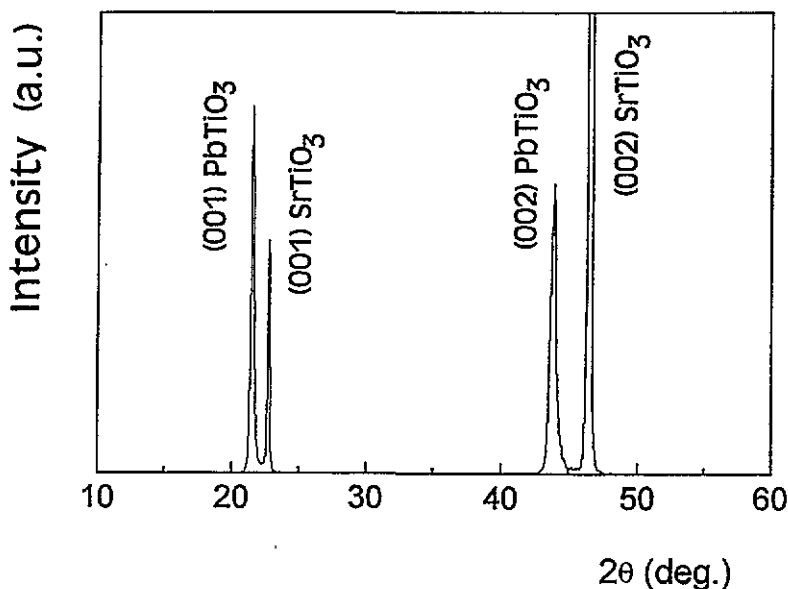


**Figure 1.** The XRD scan pattern of  $PbTiO_3$  thin films deposited on a  $SrTiO_3(001)$  substrate (a.u. arbitrary units).

$$\begin{aligned}
 & + \alpha_{112}[P_1^4(P_2^2 + P_3^2) + P_2^4(P_1^2 + P_3^2) + P_3^4(P_1^2 + P_2^2)] + \alpha_{123}P_1^2P_2^2P_3^2 \\
 & + \frac{1}{2}C_{11}(S_1^2 + S_2^2 + S_3^2) + C_{12}(S_1S_2 + S_2S_3 + S_3S_1) + \frac{1}{2}C_{44}(S_4^2 + S_5^2 + S_6^2) \\
 & - Q_{11}(S_1P_1^2 + S_2P_2^2 + S_3P_3^2) - Q_{12}[S_1(P_2^2 + P_3^2) + S_2(P_1^2 + P_3^2) + S_3(P_1^2 + P_2^2)] \\
 & - Q_{44}(S_4P_2P_3 + S_5P_1P_3 + S_6P_1P_2)
 \end{aligned} \tag{1}$$

where  $P_i$  and  $S_i$  are the polarization and strain, respectively,  $\alpha_i$ ,  $\alpha_{ij}$  and  $\alpha_{ijk}$  are the dielectric stiffness and high-order dielectric stiffness coefficients at constant stress,  $C_{ij}$  are the elastic stiffnesses and  $Q_{ij}$  are the electrostrictive constants.

The first partial derivatives of the elastic Gibbs free energy with respect to the components of  $P$  and  $S$  give their conjugate parameters the external electric field  $E_i$  and the stress  $T_{ij}$ , respectively:

$$\partial(\Delta G)/\partial P_i = E_i \tag{2a}$$

$$\partial(\Delta G)/\partial S_{ij} = T_{ij}. \tag{2b}$$

For convenience, the equations for the tetragonal state without stress and external electric field in  $PbTiO_3$  are repeated here:

$$\Delta G = \alpha_1 P_3^2 + \alpha_{11} P_3^4 + \alpha_{111} P_3^6 \tag{3}$$

$$P_1^2 = P_2^2 = 0 \quad P_3^2 = [-\alpha_{11} + (\alpha_{11}^2 - 3\alpha_1\alpha_{111})^{1/2}]/3\alpha_{111} \tag{4}$$

$$\alpha_1 = (T - \theta)/2\epsilon_0 C \tag{5}$$

$$\alpha_{11} = [-(T_C - \theta)]/\epsilon_0 C P_0^{*2} \tag{6}$$

$$\alpha_{111} = (T_C - \theta)/\epsilon_0 C P_0^{*4} \tag{7}$$

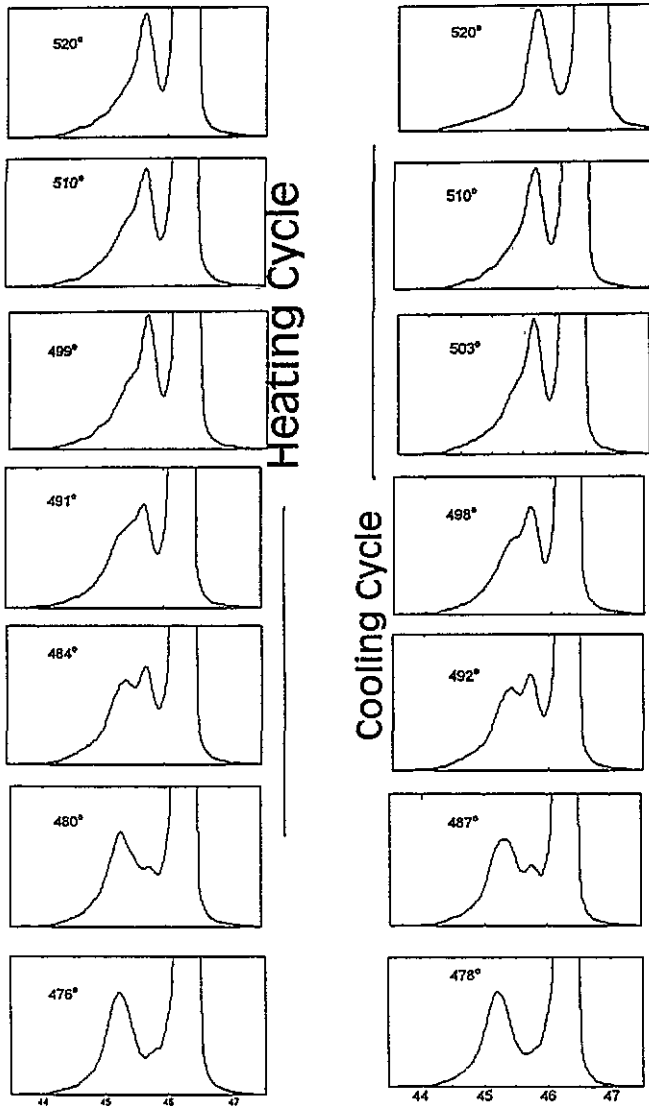


Figure 2. Temperature dependence of the XRD profile near the (002) peak of  $\text{PbTiO}_3$ .

where  $P_0^*$  is the polarization at  $T_C$ .

Considering the non-zero strains in the epitaxial thin films, additional items should be added to the original Gibbs free-energy expression and in this case only the  $c$ -axis direction strain in the as-grown thin films has been considered because of the almost zero misfit between the  $a$  and  $b$  axes of the film and substrate, so that the tetragonal solution should be written as

$$\Delta G' = \alpha_1 p_1^2 + \alpha_{11} p_3^4 + \alpha_{111} p_3^6 + \frac{1}{2} c_{33} S_3^2 \quad (8)$$

where  $S_3$  is the strain in the film.

Depending on the elastic and piezoelectric equations of  $\text{PbTiO}_3$  we have

$$\Delta P = p_3 - P_3 = d_{33} c_{33} S_3. \quad (9)$$

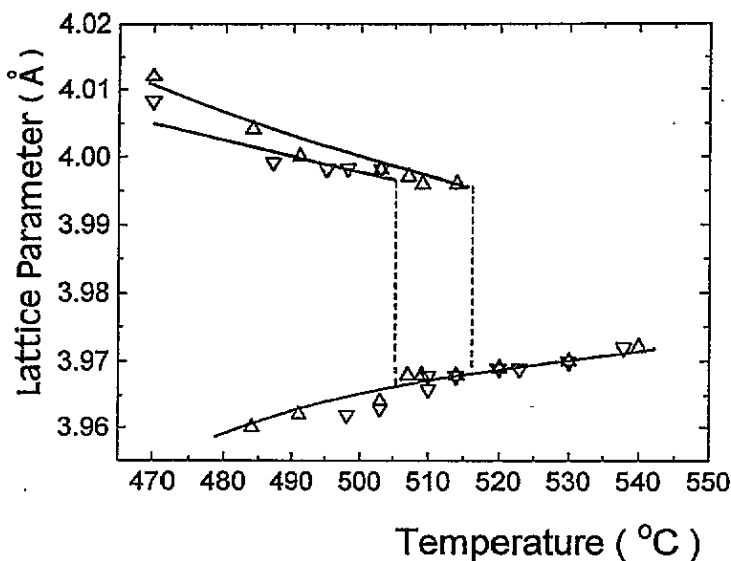


Figure 3. The temperature dependences of the lattice constants  $a$  and  $c$  of a  $PbTiO_3$  thin film:  $\Delta$ , heating cycle;  $\nabla$ , cooling cycle.

Here,  $p_3$  and  $P_3$  are the polarization in  $PbTiO_3$  with and without an additional strain, respectively. Substituting equations (8) and (9) into equation (2a) we get

$$\Delta G'/\partial p_3 = 2\alpha_1 p_3 + 4\alpha_{11} p_3^3 + 6\alpha_{111} p_3^5 + S_3/d_{33} = 0. \tag{10}$$

Now the relationship between the phase transition temperature and the deformation of the  $c$  axis has been obtained:

$$T_C = \theta + [2\alpha_1 p_3 + S_3/d_{33}]\epsilon_0 C / (4^* p_3^3 / P_0^{*2} - 3^* p_3^5 / P_0^{*4}). \tag{11}$$

Table 2. Constants used in calculation.

$\theta$ ( $^{\circ}C$ )	470
$C$ ( $10^5$ $^{\circ}C$ )	1.1
$a$ ( $\text{\AA}$ )	3.900
$c$ ( $\text{\AA}$ )	4.150
$P_0'$ ( $C\ m^{-1}$ ) at $T_C$	0.393
$P_0$ ( $C\ m^{-1}$ ) at $25^{\circ}C$	0.732
$\alpha_1$ ( $10^8\ m\ F^{-1}$ ) at $25^{\circ}C$	-2.286
$c_{33}$ ( $10^{10}\ N\ m^{-2}$ )	3.25
$d_{33}$ ( $10^{-12}\ C\ N^{-1}$ )	117

The Curie temperature is a characteristic parameter of a material and does not change with the external influence. All constants used in the calculation are listed in table 2. The strain in the  $c$  direction of the as-grown  $PbTiO_3$  thin film is about 1.16% determined by experiment; so the calculated phase transition temperature using equation (11) is  $506.7^{\circ}C$ . A plot of the calculated  $T_C$  versus the strain in the thin film is shown in figure 4; it is clear

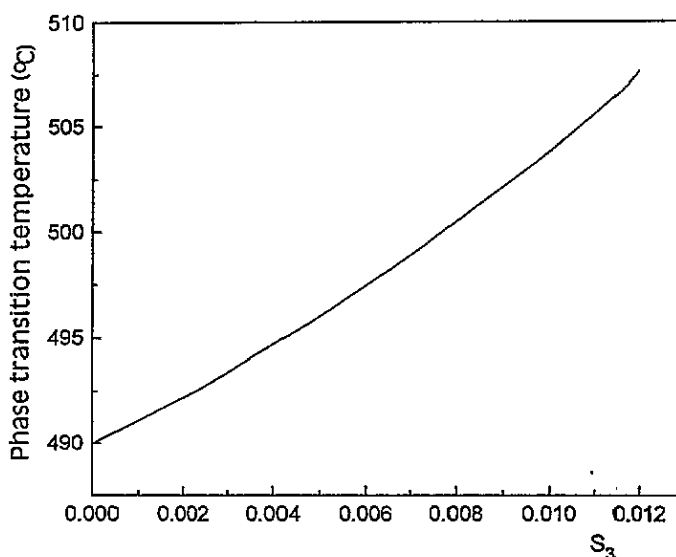


Figure 4. The calculated phase transition temperature versus  $c$ -axis strain plot of a  $\text{PbTiO}_3$  thin film on a  $\text{SrTiO}_3$  substrate.

that the phase transition temperature upshift for  $\text{PbTiO}_3$  is proportional to the strain in the epitaxial film.

From the physical viewpoint we know that, when the lattice misfit between the deposited film and substrate is small, the interface between them is coherent and the film and substrate tend to have similar lattice structures to reduce the interface energy; under this condition the film has a preferential orientation instead of random orientations and we obtain epitaxial films. It is supposed that the epitaxial thin films suffered a force created by the substrate and in this case the  $\text{PbTiO}_3$  film suffered an attractive force so that the  $c$ -axis length becomes shorter. We believe that this can lessen the abrupt change in the two sides to the interface and is favourable in lowering the total free energy of the film and the substrate. This special force between the epitaxial film and substrate should be the Coulomb force, but its details need further research.

The above consideration of the relation between the strain and phase transition temperature in an epitaxial thin film is the simplest case because there are no strains in the  $a$  or  $b$  directions in the  $\text{PbTiO}_3$  film deposited on a  $\text{SrTiO}_3$  substrate; when there are misfits in these two directions, other strain and coupling items should be considered. For a more complex case, such as polycrystalline films, the crystalline boundary energy should also be included and these elements should also cause a change in the film phase transition temperature.

#### 4. Conclusion

A  $\text{PbTiO}_3$  film in which  $a$  and  $c$  domains coexist has been deposited on a  $\text{SrTiO}_3(001)$  substrate; the XRD  $\phi$  scan proved that the in-plane vectors of the film are aligned with the corresponding vectors of the substrate and that the film is epitaxial. In this epitaxial film, the  $\text{PbTiO}_3$  cells tend to have the same structure as the  $\text{SrTiO}_3$  substrate; so the  $\text{PbTiO}_3$

has a shorter *c*-axis length; we attribute this difference to the influence of the substrate. Using the Landau–Devonshire phenomenological theory, we consider an additional strain item in the free energy of the film contrast to its normal expression in the bulk single crystal; this causes an increase in the phase transition temperature. The calculated phase transition temperature agreed well with the experimental value.

### Acknowledgment

This work is supported in part by the National 863 High Technology Program of the People's Republic of China.

### References

- [1] Swartz S L and Wood V E 1992 *Condens. Matter News* **1** 4
- [2] Scott J F and Paz De Araujo C A 1989 *Science* **246** 1400
- [3] Vest R 1990 *Ferroelectrics* **102** 53
- [4] Manasevit H M 1968 *Appl. Phys. Lett.* **12** 156
- [5] Kwak B S, Boyd E P and Erbil A 1988 *Appl. Phys. Lett.* **53** 1702
- [6] Swartz S L, Seifert D A, Noel G T and Shrout T R 1989 *Ferroelectrics* **93** 37
- [7] Gao Y, Bai G, Merkle K L, Chang H L M and Lam D J 1993 *Thin Solid Films* **235** 86
- [8] Okada M, Takai S, Amemiya M and Tominaga K 1989 *Japan. Appl. Phys.* **28** 1030
- [9] Erbil A, Braun W, Kawk B S, Wilkens B J, Boatner L A and Budai J D 1992 *J. Cryst. Growth* **124** 684
- [10] Chen Y F, Yu T, Chen J X, Shun L, Li P and Ming N B 1995 *Appl. Phys. Lett.* **66** 148
- [11] de Keijsers M, Dormans G J M, Cillessen J F M, de Leeuw D M and Zandbergen H W H 1991 *Appl. Phys. Lett.* **58** 2636
- [12] Bai G R, Chang H L M, Foster C M, Shen Z and Lam D J 1994 *J. Mater. Res.* **9** 156
- [13] Zhong W L, Wang Y G, Kong D S, Zhang P L and Qu B D 1994 *Thin Solid Films* **237** 160
- [14] Bai G R, Chang H L M, Foster C M, Shen Z and Lam D J 1994 *J. Mater. Res.* **9** 156
- [15] Iijima K, Tomita Y, Takayama R and Ueda I 1986 *J. Appl. Phys.* **60** 361
- [16] Chen Y F, Chen J X, Shun L, Yu T, Li P, Ming N B and Shi L J 1995 *J. Cryst. Growth* **146** 624
- [17] Amin A, Haun M J, Badger B, McKinstry H and Cross L E 1985 *Ferroelectrics* **65** 107
- [18] Haun M J, Furman E, Jang S J, McKinstry H and Cross L E 1987 *J. Appl. Phys.* **62** 3331
- [19] Devonshire A F 1949 *Phil. Mag.* **40** 1040
- [20] Devonshire A F 1951 *Phil. Mag.* **42** 1065